A sorting nexin 3 retromer regulates the surface localization and activity of a Wnt-activated polycystin channel complex

Shuang Feng[1][*], Andrew J Streets[1][*], Vasyl Nesin[2], Uyen Tran[3], Hongguang Nie[2], Marta Onopiuk[2], Oliver Wessely[3], Leonidas Tsiokas[2], Albert CM Ong[1]

[1]Kidney Genetics Group, Academic Nephrology Unit and the Bateson Centre, University of Sheffield Medical School, Sheffield, UK

[2]Department of Cell Biology, University of Oklahoma Health Sciences Center, 975 NE 10th Street, Oklahoma City, OK 73104, USA

[3]Department of Cellular and Molecular Medicine, Lerner Research Institute, Cleveland Clinic Foundation, Cleveland, USA

*equal contribution

Correspondence:

Albert CM Ong

Academic Nephrology Unit, Department of Infection Immunity and Cardivascular Disease, University of Sheffield, Sheffield S10 2RX, UK

Tel: +44 114 215 9542

Fax: +44 114 271 3892

Email: a.ong@sheffield.ac.uk

Running title: Retromer complex and polycystin-2

Keywords: Polycystin-2, ADPKD, PKD2, Sorting nexin-3, retromer

Total word count: 3403

Abstract

Autosomal dominant polycystic kidney disease (ADPKD), is caused by inactivating mutations in PKD1 (85%) or PKD2 (15%). The ADPKD proteins, polycystin-1 (PC1) and polycystin-2 (PC2) form a plasma membrane receptor-ion channel complex. However the mechanisms controlling the subcellular localization of PC1 and PC2 are poorly understood. The retromer complex is an ancient protein module initially discovered in yeast that regulates the retrieval, sorting and retrograde transport of membrane receptors. Here, we report for the first time that PC1 and PC2 are retromer cargos, whose surface expression and function are regulated by a sorting nexin 3 (SNX3)-retromer complex. Two SNX-3 isoforms, one novel, with distinct binding properties to PC2, were identified though yeast-2-hybrid, biochemical and cellular assays. Knockdown of SNX-3 or the core retromer protein VPS35 resulted in an increased surface expression of endogenous PC1 and PC2 in vitro and in vivo with evidence of increased Wnt-activated endogenous PC2-dependent whole cell currents. Molecular targeting of endosomal sorting of PC1 and PC2 could lead to new therapeutic approaches in ADPKD.

Introduction

Autosomal dominant polycystic kidney disease (ADPKD) is the most common inherited renal disease. It is a major cause of end-stage renal disease (ESRD) worldwide and accounts for ~10% of all patients on renal replacement therapy [1]. ADPKD is caused by germline mutations in PKD1 (type 1 ADPKD) or PKD2 (type 2 ADPKD) genes. The ADPKD proteins, polycystin-1 (PC1 or PKD1) and polycystin-2 (PC2, PKD2, or TRPP2) form a heterodimeric protein complex which is essential for maintaining tubular differentiation, polarity and diameter [2].

Despite the demonstration of a PC1-PC2 complex in heterologous or native systems[3-5], the subcellular localization of both proteins only overlaps in a few domains of the plasma membrane or the primary cilium [6]. Some studies have reported that PC2 can function independent of PC1 as a cell surface receptor-operated Ca^{2+}-permeable channel complexed with other members of the TRP superfamily of ion channels such as TRPC1 [7], TRPV4 [8, 9] or both [10]. We recently reported that the cell surface pool of PC1/PC2 in mouse embryonic fibroblasts and transfected CHO-K1 cells can be activated by Wnt proteins, suggesting that the PC1/PC2 complex can function as a ligand activated channel complex [11]. In addition to the cell surface pool of PC2, the majority of PC2, but not PC1, can be detected in the ER [4, 12], where it enhances ER Ca^{2+} release in response to G protein coupled receptors linked to the production of IP_3 as a second messenger [13, 14]. Therefore, PC2 is likely to have multiple roles in Ca^{2+} signaling depending on its subcellular localization, particularly in relation to PC1 [3, 4, 12, 15-18].

Here, we report for the first time that PC1 and PC2 are retromer cargos and the surface expression of PC2 is regulated by distinct SNX3 isoforms at the stages of clathrin-mediated endocytosis (SNX3-102) and retrograde transport and sorting (in case of the classical SNX3-162 and VPS35) in the endosomal pathway.

Results

SNX3-102, a novel SNX3 isoform, is a new interacting partner of PC2

To identify novel regulators of PC2 sorting and trafficking, we performed a yeast-2-hybrid (Y2H) screen of a mouse E17 cDNA library using a region (aa799-895) of the PC2 C-terminus (CT2) as bait. This region contains several important functional motifs including several important serine phosphorylation residues (Ser[801], Ser[812], Ser[829]), a coiled-coil domain (CC2, aa833-871) essential for CT2 dimerisation and interaction with the C-terminus of PC1 (CT1) and a heterodimerisation sequence (aa871-895) for PC1 binding [5, 17, 19]. Among several positive interactors (data not shown), we identified SNX3-102, a novel isoform of SNX3. We confirmed its interaction to CT2 (aa 680-968) in directed yeast-2-hybrid assays (Fig 1a). Mutation of CC2 (4M) which disrupts CT2 dimerization and PC1 recognition [5], however had no effect on binding. Interestingly, CT2 did not bind to the classic SNX3 isoform (SNX3-162, isoform 1) (Fig 1a). To confirm that the interaction between SNX3-102 and CT2 was direct, we carried out in vitro GST pull-down assays using recombinant GST-SNX3 and Thio-CT2 proteins. Consistent with yeast 2-hybrid assays, GST-SNX3-102 but not GST-SNX3-162 showed direct binding to both Thio-CT2 (799-871) (not shown) and Thio-CT2 (680-968) (Fig 1b).

Sequence analysis revealed that compared with SNX3-162, SNX3-102 lacked exon 3 and a part of exon 4 due to alternative splicing at a cryptic splice site (Fig 1c, Supp Fig 1). This deletes most of the PX domain (aa27-151). Since four other SNX3 isoforms have previously been reported, we have named this new isoform as isoform 5. Q-PCR analysis of developing mouse embryos (E10-E16) and a number of mouse and human kidney cell lines confirmed that SNX3-102 is widely expressed but at much lower levels (3-5%) relative to SNX3-162 (Fig 1d) or other kidney cell lines (Supp Fig2c).

The disrupted PX domain in SNX3-102 cannot mediate phospholipid binding

We next performed co-immunoprecipitation experiments to confirm the interactions between full-length SNX3-102 and PC2. Using HEK293 cells, SNX3-102 co-immunoprecipitated with PC2 (Fig 2a). Unexpectedly, binding was also observed with SNX3-162 (Fig 2a). This raised the possibility of an indirect interaction or binding to a different domain of PC2. To better understand this discrepancy, we decided to better

characterise SNX3-102. SNX3-162 has been shown to be recruited to endosomes in a PtdIns(3)P dependent manner [20]. Binding has been demonstrated to be mediated by a PX domain though evidence of a second non-canonical PtdIns(3)P binding site in the C-terminus (aa147-162) has also been reported [21]. To determine whether the missing exons in SNX3-102 were functionally important for phospholipid binding, protein-lipid overlay assays were carried out using commercial lipid strips. As predicted, GST-SNX3-162 bound strongly to PtdIns(3)P and weakly to PtdIns(5)P (Supp Fig 2a). In contrast, GST-SNX3-102, showed no lipid binding under the same conditions. These results are in line with the hypothesis that the intact PX domain is essential for phospholipid binding (and endosomal recruitment). Thus SNX3-102 is likely function in a different compartment from that of SNX3-162.

The subcellular localization of SNX3-102 and SNX3-162 are distinct

Expression of GFP-tagged SNX3 isoforms in several cell lines revealed a striking difference in their localization. GFP-SNX3-162 showed a strong overlapping distribution to EEA1-positive early endosomes whereas GFP-SNX3-102 co-localized with adaptor protein-2 (AP2) which is enriched in clathrin-coated endocytic vesicles (Fig 2b). Consistent with this, we observed GFP-SNX3-102 expression at or close to the plasma membrane in the majority (70% or more) of transiently transfected cell lines including HeLA, MDCK, LLC-PK1 and IMCD3 (Fig 2b and data not shown). Taken together, these results suggest that SNX3-102 could be involved in AP2 or clathrin mediated endocytosis of PC2 whereas SNX3-162 is involved in its retrograde transport and sorting in early endosomes. GST pull-down assays from HEK293 using co-expressed GST-SNX3-102 revealed specific interactions with endogenous clathrin heavy chain (CHC) and the AP2 μ2 (AP2M1) subunit (Fig 2c). In contrast, GST-SNX3-162 did not interact with either protein consistent with its localization to early endosomes.

The retromer complex protein VPS35 binds directly to the N-terminus of PC2

Since SNX3-162 was localized to early endosomes and could associate with full-length PC2, we investigated the possibility that it could bind to either N- or C-terminus of PC2

(NT2 or CT2) indirectly via the retromer complex. The retromer complex originally identified in yeast comprises two sub-complexes: a trimer (Vps26-29-35) which functions as a cargo-selective adaptor and a membrane deforming sub-complex consisting of a SNX-BAR heterodimer. We found that the full-length HA-PC2 and GFP-VPS35 proteins co-immunoprecipitated when expressed in HEK293 cells (Fig 2d) and confirmed that endogenous PC2, VPS35 and SNX3-162 were present in the same complex in LLC-PK1 cells (Fig 2e). Significantly, knockdown of endogenous VPS35 abolished the binding between PC2 and SNX-162 in LLC-PK1 (Fig 2f, Supp Fig 2e). To define the binding domain in PC2 mediating the interaction with VPS35, GST pull-down assays from whole cell extracts were next performed. This revealed a clear interaction between GFP-VPS35 and GST-NT2 (aa1-223) but not with GST-CT2 (aa680-968) (Fig 2g). Finally, we confirmed that the interaction between NT2 and VPS35 was direct using a recombinant protein containing the entire VPS35, VPS26 and VPS29 trimer (Fig 2h).

To investigate whether the involvement of the retromer complex in PC2 trafficking could be extended to PC1, we investigated the interaction between VPS35 and the C-terminus of PC1 (CT1). In HEK293 cells, binding between GFP-VPS35 and GST-CT1 (aa4107-4303) was detected (Fig 2g). Similar to NT2, we confirmed a direct interaction between recombinant MBP-CT1 and the FLAG-VPS35/26/29 proteins in vitro (Fig 2i). Interestingly, co-immunoprecipitation could not be confirmed between GFP-VPS35 and full-length PC1 (not shown) suggesting that the interaction between the full-length proteins could be conformationally restricted or depend on the presence of PC2 in vivo. Our results however are consistent with PC2 being a direct retromer cargo.

Knockdown of SNX3 or VPS35 increases PC2 surface expression

Since our data suggested a potential role for SNX3 in the recycling of plasma membrane PC2, we hypothesised that knockdown of endogenous SNX3 would affect the surface expression of endogenous PC2. In previous studies, we and others had shown that in kidney epithelial cells, the vast majority of PC2 is localized in the ER, but a small percentage of PC2 (less than 10%) can be detected at the plasma membrane and ciliary membrane [4, 7, 18,]

[22]. This cell surface pool of PC2 is functional, since it has been shown to contribute to basal conductance and can be further activated by EGF, G protein coupled receptor agonists [23] and Wnt ligands [11] in diverse cell types.

Efficient knockdown of both SNX3 isoforms was achieved using sequence specific siRNA in LLC-PK1 cells (Supp Fig 2b,d). As the endogenous expression of SNX3-102 was not easily detectable by immunoblotting, we confirmed knock-down of this isoform at the mRNA level by semi-quantitative RT-PCR using isoform specific primers (Supp Fig 2b). Significantly, we observed an increase in surface PC2 and PC1 following SNX3 knockdown by both surface biotinylation (Fig 3a,b) and of PC2 by immunofluorescence labelling (Fig 3d,e). Unfortunately, increased cell surface expression of endogenous PC1 by indirect immunofluorescence could not be achieved, because several available PC1 antibodies did not work in this assay. However, deglycosylation analysis of surface labelled PC1 and PC2 complex confirmed that surface labelled PC1 was EndoH-resistant whereas labelled PC2 remained fully EndoH-sensitive (Fig 3c). As expected, the membrane protein Na^+ K^+ ATPase was EndoH-resistant in the same assay (Fig 3c).

To substantiate our findings, we next depleted endogenous VPS35 by siRNA. Similar to SNX3, this resulted in a marked effect on surface PC1 and PC2 expression by surface biotinylation (Fig 3a,b) and of PC2 by immunofluorescence labelling (Fig 3d,e). This effect was even more pronounced than the knockdown of SNX3 (both isoforms). Finally, we did not observe detectable changes in ciliary expression of PC2 following knockdown of SNX3 or VPS35 (Fig 3d). Taken together, these results suggest that PC2 and PC1 recycling to the plasma membrane is likely to be mediated to a large extent by the SNX3-162-VPS35 interaction at the level of early endosomes.

Knockdown of VPS35 in Xenopus embryos increases PC2 surface expression in pronephric kidney tubules

To examine whether inhibition of the retromer complex had a similar effect on PC2 localization in vivo, we turned to Xenopus as a model for PKD [24, 25]. In Xenopus, PC2 is

expressed along the entire length of the pronephric kidney and the protein can be detected by immunofluorescence confocal microscopy both at the cell membrane and the apical cilia (Fig 3f, Supp Fig 3a) [24]. To inhibit the retromer complex, embryos were injected at the 2-cell stage with an antisense morpholino oligomer targeting VPS35 (VPS35-MO), which has been characterized previously [26]. At late tail bud stage, knockdown of VPS35 confirmed at the protein level (Supp Fig 3c) resulted in increased staining for PC2 protein in kidney tubules at the cell membrane both apically and basolaterally (Fig 3f). This was confirmed by quantification of the apical PC2 signal in the proximal tubules using counterstaining with Erythrina Cristagalli Lectin (ECL, Fig 3g). Finally, as expected from the ubiquitous expression of Vps35, the upregulation of PC2 protein was not limited to the pronephric kidney only, but was also be observed in other tissues expressing PC2 (e.g. notochord, data not shown).

Knockdown of VPS35 increases Wnt activated PC2 whole cell current density

Next, we tested whether retromer function could regulate Wnt activated PC2-dependent Ca^{2+} signaling. In a recent paper, we showed that purified Wnt9b induced large PC2-dependent whole cell currents in mouse embryonic fibroblasts (MEFs) and transfected CHO-K1 cells [11]. Here, we tested whether Wnt9b could also induce endogenous PC2-dependent whole cell currents in LLC-PK1 cells. We confirmed that LLC-PK1 expressed endogenous PC1 (Supp Fig 4a) and responded to Wnt9b in a dose-dependent manner. Time course experiments using purified Wnt9b (12.5 nM for a 40 kDa protein) induced time-dependent and La^{3+}-inhibited whole cell currents (Fig 4a-c). Dose-response experiments indicated that Wnt9b or Wnt5a activated whole cell inward (-100 mV) and outward (+100 mV) currents with values ranging from 45 to 76 ng/ml (Supp Fig 4b). This effect was dependent on endogenous PC2 as knockdown of PC2 completely suppressed the response to Wnt9b [27]. (Fig 4d-f).

Upon depletion of VPS35, Wnt9b (500 ng/ml) induced whole cell current density was ~2-fold larger (Fig 4g-i) than current density induced by Wnt9b in mock-transfected cells (Fig 4a-c). To test whether PC2 contributed to Wnt9b-induced currents in VPS35-depleted cells,

PC2 was downregulated together with VPS35. Doubly-transfected cells showed diminished response to Wnt9b (Fig 4j-l), indicating that the increased magnitude in Wnt9b-induced currents in VPS35-depleted cells was due to a specific upregulation of plasma membrane PC2. Wnt5a showed a similar effect to Wnt9b (Supp Fig 4b). Summary data for inward and outward current densities are shown in Fig 4 (m, n). Because VPS35 knockdown could potentially affect the trafficking of other channels to and from the plasma membrane, we compared cell capacitance in mock and VPS35-depleted cells. We however, could not record a measurable difference in total cell capacitance between the two cells types (Fig 4o) indicating that depletion of VPS35 did not have a substantial effect on the trafficking of other channels to and from the plasma membrane. We were unable to test the effect of SNX3 knockdown on PC1/PC2 channel activity as whole cell currents were unstable for electrophysiology experiments. Overall, these studies showed that depletion of VPS35 did not only increase the cell surface expression of PC2 protein, but also PC2-dependent whole cell currents.

Discussion

The SNXs are a family of proteins first identified in yeast which share a Phox (PX) domain with affinity for PtdIns(3)P. In mammals, at least 33 SNXs have been identified [28]. In yeast, the best characterized function of the retromer complex is to regulate retrograde transport of cytosolic proteins from late endosomes to the TGN (trans-Golgi Network). In mammalian cells however, the functions of the retromer complex are now thought to be broader since components of the retromer complex are found throughout the endosomal network (including clathrin-coated vesicles) [29], early endosomes (EGF receptor retrieval) [20, 30] with enrichment in sorting endosomes where decisions on the fate of endocytosed cargo towards rapid recycling (to the plasma membrane), degradation (in lysosomes) or recycling (via the TGN) are made. Recently, a non-classical retromer complex consisting of the VPS26-29-35 trimer associated with monomeric SNX3 (rather than with a SNX-BAR heterodimer) was reported [31, 32]. This SNX3 retromer was shown to be essential for Wnt secretion in C. elegans and D. melanogaster through regulating the retrograde transport of Wntless and was preferentially localized in early endosomes rather than sorting

endosomes where SNX-BAR retromer complexes are enriched [32]. This spatial segregation could favor sequential cargo handling between both retromer complexes. Our discovery of a novel SNX3 isoform (SNX3-102) refines the role for SNX3 in this pathway by linking clathrin-mediated endocytosis to early endosomes (Figure 5).

Here we report for the first time that PC1 and PC2 are hitherto unrecognized cargos of a SNX3-retromer complex and demonstrate that VPS35 regulates the surface expression of PC1 and PC2 in vitro and in vivo. An initial yeast-2-hybrid screen using the C-terminus of PC2 as bait identified a novel isoform of SNX3 as a direct PC2 binding partner. We have named this isoform 5. The new isoform (SNX3-102) is likely to be generated by alternative splicing since it excludes exons 3 and part of exon 4 and consequently lacks most of the predicted PX domain found in the classical isoform 1 (SNX3-162). However quantitative gene expression analysis has shown that it is expressed at much lower levels (5%) compared to isoform 1. Strikingly, SNX3-102 was predominantly localized to clathrin-coated vesicles, where it co-localized with AP2. This is in contrast to SNX3-162 which was predominantly localised in EEA-1 positive early endosomes. Based on our interaction studies, these findings suggest that PC2 is endocytosed by clathrin-AP2 mediated binding. This observation was confirmed by the fact that SNX3-102, but not SNX3-162 bound to the endogenous clathrin heavy chain (CHC) and the AP2 μ2 (AP2M1) subunit in HEK293 cells. However, our results do not exclude possible roles for the other SNX3 isoforms (isoforms 3 and 4 but not 2) which would also have been targeted by the SNX3 siRNA used (Fig 1c).

Importantly, we showed that LLC-PK1 cells depleted of VPS35 showed an increase in Wnt9b-induced current density directly proportional to the increase in the cell surface expression of endogenous PC2 in these cells. Given the fact that PC2 cannot form a Wnt-activated channel without PC1, our data indicate that the limiting factor in PC1/PC2 channel function is PC2 in LLC-PK1 cells. Despite significant efforts, we could not obtain stable currents in cells depleted of SNX3, suggesting that structural changes in the plasma membrane could have affected the quality of the plasma membrane required for reliable

current measurements.

An important observation was that the SNX3-retromer complex regulated surface expression and function of PC1 and PC2 at the plasma membrane but did not regulate cilia localization of PC2 and by inference the function of the cilia PC1/PC2 complex. This is not unexpected since distinct mechanisms regulating the forward trafficking of PC2 to either cilia or plasma membranes have also been described [33]. Whilst there is agreement that PC2 is present in several subcellular compartments such as the ER, endosomes, basolateral plasma membrane and ciliary membrane, there is inconclusive evidence that an exclusive function in any one compartment (including primary cilia) is sufficient to prevent cystogenesis [2, 5, 34]. Indeed, reduced cilia PC2 due to impaired Golgi sorting (GMAP210 null mice) [35, 36] or absent cilia PC1 due to defective PC1 cleavage (Pkd1$^{\text{v/v}}$ mutant mice) [37, 38] did not result in an early-onset PKD phenotype in vivo suggesting that different functional pools of the PC1/PC2 complex are important during kidney development, in different tubular segments [37] and by inference, in the mature organ [34]. In addition, since our experiments were not conducted under conditions that promoted optimal cilia formation, it is probable that the Wnt-activated Ca^{2+} currents we measured can be attributed to plasma membrane PC1/PC2 and not the cilia PC1/PC2 complex. This is in agreement with recent work suggesting that the PC1/PC2 cilia signal is unlikely to be activated either by flow or mediated by Ca^{2+} [39]. Also, since we were unable to identify an EndoH-resistant PC2 cilia fraction reported by one group [38], our observations are most likely relevant to the plasma membrane PC1/PC2 fraction [4, 40].

In summary, our results support a sequential model where SNX3-102 first regulates PC2 endocytosis by directly binding PC2 and AP2/clathrin to cluster PC2 in clathrin-coated vesicles before relaying it to early endosomes where SNX3-162 and VPS35 regulate its sorting and fate, together with that of PC1 (Fig 5). In a recent paper, we have reported an alternative pathway for PC1/PC2 endocytosis via an AP2/ARBB1 mechanism mediated by direct binding to the PC1-PLAT domain; here however, endocytosis from plasma membrane and cilia membranes were similarly affected and dependent on PKA-

phosphorylation of PLAT at a specific residue (Ser^{3164}) [41]. The precise relationship between these two retrieval pathways is unclear but likely represent both constitutive (VPS35-PC2) and regulated (ARBB1-PC1) mechanisms. In any case, we suggest that that a disruption in retrograde transport to the TGN and possibly clathrin-mediated endocytosis leads to increased surface delivery of PC1 and PC2 by promoting rapid recycling from early endosomes. Finally, our study could have potential therapeutic applications. It is possible that compounds that down-regulate SNX3 or VPS35 expression or which inhibit their recruitment or function [21, 30] could have therapeutic benefit in ADPKD patients with hypomorphic mutations by enhancing PC1/PC2 surface expression.

Materials and methods

All chemicals were purchased from Sigma (Poole, UK) unless otherwise stated. Antibodies were purchased from the following suppliers: Mouse anti-Thio (Invitrogen), Mouse anti-GST (Serotec), Mouse anti-Clathrin HC (BD Biosciences), Rabbit anti-SNX3 (Abcam), Mouse anti-EEA1 (BD Biosciences), Goat anti-PC2 (G20) (Santa Cruz), Mouse anti AP2 $\mu 2$ subunit (AP50, BD Biosciences), Rat anti-HA (Roche), Rabbit anti-HA (Santa Cruz), Rabbit anti-c-Myc (Santa Cruz), Rat anti-c-Myc (Serotec), Mouse anti-Pk/V5 (Serotec), Mouse anti-Flag (Sigma) and Mouse anti-MBP (NEB). The AP2 mAb (AP6) was the kind gift of E. Smythe (University of Sheffield). Purified Wnt9b and Wnt5a were obtained from R&D in the carrier-free formulation.

pET23d-3xFLAG retromer (FLAG-VPS35-26-29-His) and pIRES-neo-GFP-VPS35 plasmids were kind gifts of F. Kishi (Kawasaki Medical School, Okayama, Japan). cDNA of SNX3-162 and a C-terminal EGFP vector (pDG0) were gifts of E. Kiss-Toth (University of Sheffield) and K. Ross (Liverpool John Moores University, Liverpool, UK).

DNA constructs and site-directed mutagenesis.

Unless otherwise stated, the PKD2 and PKD1 plasmids used in this paper have been previously reported. N-terminal c-Myc tagged SNX3-102 and SNX3-162 constructs were generated by PCR and ligation into pcDNA3. GFP-tagged SNX3-102 and SNX3-162 were prepared by TOPO cloning into the Gateway® vector pD-G0. SNX3-102 and SNX3-162 were subcloned into pGEX-6P-1 or pEBG vectors to express N-terminal bacterial or mammalian GST-fusion proteins respectively. Similarly, NT2 (PKD2 aa1-223), CT2 (PKD2 aa680-968) and CT1 (PKD1 aa4107-4303) were subcloned into pEBG to express GST fusion proteins in mammalian cells. Site specific mutations were introduced using the Quick-change site-directed mutagenesis protocol (Stratagene) as previously described and verified by sequencing.

Yeast Two-Hybrid assays

A region of the PC2 C-terminus (CT2 799-895) was cloned into the bait vector pGBKT7 (Clontech) as previously reported [5]. This was transformed into the yeast strain AH109 (containing ADE2, HIS3 and LacZ reporter genes under the control of the GAL4 UAS) and used to screen an E17 mouse cDNA library pre-transformed in the yeast strain Y187 (Clontech). Screening was performed by a yeast-mating method using the yeast strains AH109 (MATa) and Y187 (MATα). Reporter genes HIS3 and ADE2 and LacZ were employed for triple selection of positive transformants. Directed yeast 2-hybrid assays were carried out by co-transforming bait and prey plasmids into AH109 as previously described [42]. The plasmids pGBKT7-53 (p53) and pGBADT7-T (SV40 T-antigen) were used as a pair of positive controls. The PC1 and PC2 truncated constructs pGBAD-B-CT1 (4107-4227) and pACT2-B-CT2 (680-742) were used as a pair of negative controls as previously reported.

Recombinant protein preparation

Plasmids were transformed into the E. coli strain BL21-RIPL and recombinant protein expression was induced at 37°C for 3 h with 0.5mM IPTG. Expression and purification of the FLAG-tagged retromer complex was performed as previously described [43]. GST fusion proteins and His-tagged proteins were purified with Nickel or Glutathione-Sepharose columns respectively as previously described [5].

GST pull-down assays

1-2 μg of the bacterial GST fusion protein and the His-Thio tagged potential partner protein (1-2 μg) were incubated in 300 μl binding buffer (1×TBST with 0.2 % Tween20) for 1 h at RT with gentle rotation. 40 μl of 50 % Glutathione Sepharose 4B beads (GE Healthcare) was then added and the mixture incubated with rotation for an additional hour. The beads were sedimented by centrifugation at 6000 rpm for 2 min and washed up to 6 times with 1ml volumes of ice-cold PBS. Bound proteins were eluted either using 25 μl of elution buffer or by boiling for 5-10 min in reducing sample buffer. The same procedure was followed for pull-down of mammalian GST-fusion proteins from cell lysates. Mammalian GST proteins bound to glutathione beads were similarly prepared for in vitro binding

assays except that the beads were washed up to 6 times with 1ml of ice-cold PBS, resuspended in 1xTBST (0.2% Tween20) prior to the addition of recombinant protein. Coomassie staining showed that the predominant bands eluted from the beads after incubation with cell lysates corresponded to the respective GST fusion proteins.

In vitro MBP pull-down assays

2µg of MBP or MBP-CT1 and 2µg of recombinant FLAG tagged retromer complex (3×FLAG- VPS35, VPS26, VPS29-His6) was added to 300µl of binding buffer (5mM HEPES pH7.9, 150mM NaCl, 1.5mM MgCl2, 0.1mM EDTA, 0.1% NP-40) and incubated at RT with gentle rotation for 4 h. 60µl of 50% amylose resin was then added and the mixture incubated for a further 2 h. The beads were then sedimented by centrifugation at 4ºC, washed six times with 1.5ml amylose column washing buffer to remove unbound proteins. Bound proteins were then eluted from the washed beads into loading buffer and clarified supernatants analyzed by SDS-PAGE and western blotting.

Protein-lipid overlay assays

Commercial lipid strips (Echelon® PIP strips P-6001) were blocked with 1% nonfat-dry milk in PBS (pH7.4) for one hour at RT, followed by incubation with recombinant protein in 1% nonfat-dry milk in PBS (pH7.4) at 4ºC overnight with gentle agitation. The membrane was washed in 1×PBST buffer (0.1% v/v Tween-20) for 3×10 min and bound protein detected by immunodetection.

Quantitative Real time-PCR

Normal mouse embryos (kind gift of A Furley, University of Sheffield) at different developmental stages (E10, E12, E14, E16) were pooled (n=3) and homogenized for RNA extraction. Total RNA was isolated from the embryos or cultured cells using TRIzol® (Invitrogen). Each sample was then treated with Ambion® DNA-free™ DNase kit to remove contaminating DNA. 0.8ug of DNase digested total RNA was reverse transcribed into cDNA using a cDNA reverse transcription kit (AB Applied Biosystems) according to the manufacturer's instructions. Specific primers were designed to amplify

SNX3-102 and SNX3-162 independently from human and mouse samples: primer details are provided below:

human SNX3(162), forward, 5'-CACTTACGAAATCAGGGTCAAG-3';

human SNX3(162), reverse, 5'- GGAACTACGACCTTGCTCT-3';

human SNX3(102), forward, 5'- CACTTACGAAATCAGGGTCAAG-3';

human SNX3(102), reverse, 5'- CTATTATTTCATCCTTGCTCTCTC-3';

mouse SNX3(162), forward, 5'- CACCTACGAGATCAGGGTCAAG-3';

mouse SNX3(162), reverse, 5'- GGAACTACAACCTTGCTCTCTC-3';

mouse SNX3(102), forward, 5'- CACCTACGAGATCAGGGTCAA-3';

mouse SNX3(102), reverse, 5'- CTATAATTTCATCCTTGCTCTCTC-3'.

Real time PCR was performed using the IQ^{TM} Cybr Green system (BioRad). HPRT (hypoxanthine guanine phosphoribosyl transferase) was used as housekeeping gene and the data of CT value was calculated in relation to HPRT. To analyze the data, a ΔΔCt method was used to calculate the relative mRNA level.

Cell culture and transfection

HEK-293, IMCD3, MDCKII, Hela and LLCPK cells were cultured in DMEM supplemented with 10% fetal bovine serum. Transient transfection was carried out on cells cultured to 60-80% confluency using Genejuice transfection reagent (Novagen) or Lipofectamine 2000 (Invitrogen) according to the manufacturer's instructions.

Protein biochemistry

Cells were lysed by extraction at 4°C using the IP lysis Buffer (25mM NaCl, 150mM EDTA, 1mM 0.5% NP40, 1 % Triton X-100, pH 7.0) supplemented with a protease inhibitor cocktail (Roche). Immunoblotting and immunoprecipitation (IP) were performed as previously described.

Immunofluorescence staining

Cells were grown on coverslips and fixed with 7:3 Methanol/acetone or 4% paraformaldehyde at RT for 10 min followed by air drying for 10 min. Blocking was carried out for 20 min with 5% BSA/PBS, and incubated with primary antibody overnight at 4°C in 5% bovine serum albumin/PBS. Controls included cells stained with primary antibody omitted. Antibody binding was visualized using fluorescein isothiocyanate-conjugated donkey anti-goat IgG secondary antibody (Santa Cruz, USA). Slides were viewed using an Imaging Systems inverted IX71 microscope (Olympus, Tokyo, Japan) configured for multifluorescence image capture. Images were acquired using SimplePCI imaging software (Compix, Hamamatsu, PA). For PC2 surface expression, images were quantified by identifying regions of surface staining on individual cells (n=30 for each transfection) and determining surface staining intensity using ImageJ analysis software (NIH).

siRNA knockdown

Isoform-specific siRNA to pig SNX3 was chemically synthesized by Ambion (Austin, TX) according to the following sequence: (sense: 5'-GCUUCGAAGUGAAUUAGAATT-3', antisense 5'-UUCUAAUUCACUUCGAAGCCA-3'). This targets a sequence common to isoform 1, 3, 4 and 5 (Figure 1c). A scrambled negative control siRNA (Silencer) was purchased from Ambion. For knockdown of endogenous VPS35 in LLC-PK1 cells, the following sequences were synthesised: VPS35 siRNA 1: 5'-UAAAGAUACAACAUCCUCUGAAGGC-3' and VPS35 siRNA 2: 5'-GCCUUCAGAGGAUGUUGUAUCUUUA-3'. Transfection of 20 nM siRNA into cells was achieved using RNAimax reagent (Invitrogen). The efficiency of knockdown was assessed by immunoblotting or RT-PCR 72 h post-transfection.

Cell surface biotinylation

Cells were cultured to 90% confluence in 6 well dishes, washed three times with PBS and incubated for 40 min with 1 mg/ml sulpho-NHS-SC-Biotin in PBS pH 8.0 at 4°C. Cells were rinsed twice with PBS containing 100 mM glycine and excess biotin quenched by further incubation for 20 min with PBS containing 100 mM glycine and 0.1% BSA. After

washing twice with PBS, they were lysed in 500 µl buffer (50 mM Tris, 500 mM NaCl, 5 mM EDTA, 1% TX-100, pH 7.5) for 1 h at 4°C. Equal amounts of cell lysate were incubated with 100 µl streptavidin beads overnight at 4°C. Beads were washed three times each with lysis buffer, high salt buffer (50 mM Tris, 500 mM NaCl, 0.1% TX-100) and non-salt buffer (10 mM Tris, pH 7.5) before being resuspended in 40 µl 2×SDS sample buffer. Samples were analysed by SDS-PAGE and western blotting using the antibodies described and bands quantified using a Biorad Gel Doc XR+ Imager.

EndoH deglycosylation

Following cell surface biotinylation, labelled proteins were incubated with 500 Units EndoH (New England Biolabs, UK) as previously described [4].

Xenopus Embryo Manipulations

Xenopus experiments were approved by the Institutional Animal Care and Use Committee and adhered to the National Institutes of Health Guide for the Care and Use of Laboratory Animals. Embryos obtained by in vitro fertilization were maintained in 0.1x modified Barth medium [44] and staged following [45]. Knockdown of Vps35 was performed using an antisense morpholino oligomer (Vps35-MO, 5'-GGA CTG CTG GGT CGT GGG CAT CAT C'-3', GeneTools) previously reported in Coudreuse et al. [26] and confirmed by immunoblotting using a validated Vps35 antibody (ab154647, Abcam). Injections were performed at the 2-cell stage targeting a single blastomere with the contralateral side serving as uninjected control. Embryos were analyzed when sibling uninjected control embryos reached stage 40.

For immunofluorescence analysis embryos were fixed in Dent's fixative (Methanol:DMSO=4:1). Xenopus embryos were then embedded in paraplast and sectioned at 25 µm. Sections were probed with an antibody recognizing Xenopus PC2 (#AB9088, EMD Millipore, see Supplementary Figure S2 for antibody validation) and visualized by staining with anti-rabbit Alexa-647. Sections were counterstained with DAPI and Erythrina Cristagalli Lectin (ECL, Vector Laboratories) to visualize nuclei and the apical domain of

the proximal tubules as described previously [46]. Slides were analyzed by confocal microscopy and apical PC2 staining was quantified using ImageJ determining the number of pixels within the ECL staining domain.

Electrophysiology

LLC-PK1 cells were co-transfected with a porcine VPS35-specific siRNA 1 (see sequence above) or porcine PC2-specific (sense: 5'-UGUAGUAGUACACUGGAGC-3') siRNA and CD8α using Lipofectamine 2000 (Invitrogen). Transfected cells were identified using anti-CD8α-coated beads (DYNAL). CD8α plus a scrambled siRNA (sense: 5'-UUCUCCGAACGUGUCACGU-3', Qiagen) were used in mock-transfected cells. Transfection reactions were performed in 35-mm dishes using 1μg DNA (CD8α cDNA) and 40 pmoles of one or two siRNAs (VPS35 siRNA 1 or PC2 siRNA) in a total of 500 μl media containing 6 μl Lipofectamine2000.

Immediately before each experiment, a coverslip bearing LLC-PK1 cells was removed from the culture plate and put into a recording chamber, which was mounted on the stage of a Nikon Diaphote inverted microscope. The extracellular solution was normal Tyrode solution containing (in mM): 135 NaCl, 5.4 KCl, 0.33 NaH$_2$PO$_4$, 1 MgCl$_2$, 1.8 CaCl$_2$, 5 HEPES, 5.5 glucose (pH 7.4). Recording pipettes were made from capillary glass (plain; Fisher Scientific, Pittsburgh, PA, USA) using a micropipette puller and polisher (PP-830 and MF-830, respectively; Narishige, Tokyo, Japan). Pipettes were back-filled with internal solution composed of (in mM): 100 K-aspartate, 30 KCl, 0.3 Mg-ATP, 10 HEPES, 10 EGTA, and 0.03 GTP (pH 7.2). Pipette resistance varied from 3–5 MΩ when filled with this internal solution. Offset potential was corrected just before a gigaohm seal formation. Series resistance and capacitance transients were compensated with a Warner PC-505B amplifier (Warner Instrument Corp., Hamden, CT, USA) and pClamp 10.0 software (Axon Instrument, Foster City, CA, USA). Currents were digitized with a Digidata 1440A converter (Molecular Devices), filtered through an internal four-pole Bessel filter at 1 kHz, and sampled at 2 kHz. Inward and outward whole-cell currents were elicited by employing a step-pulse protocol from -100 to +100 mV every 3 seconds for 200 millisecond duration

from a holding potential of -60 mV. Current-voltage (I-V) curves were derived using a voltage step protocol ranging from -100 to +100 mV in 20-mV increments for 200 milliseconds duration from a holding potential of -60 mV. Steady-state currents were averaged between 50 and 100 milliseconds. Cells with a similar diameter were selected for recordings, and only those cells with stable baseline currents were included in the results. Purified Wnt proteins were directly applied to the bath solution from a stock solution of 100 ng/μl.

Statistics

Data are presented as mean values ± SEM. Student's t test was used for statistical analysis with a p value of <0.05 indicating statistical significance. All analysis was carried out using Prism (Graphpad). Current traces were analyzed off-line with pClamp 10.0. All results are presented as means (± SE). One-way analysis of mean and variance computation was used to analyze data with unequal variance between each group. A probability level of 0.05 was considered significant. The Boltzmann equation used to plot $I_{normalized}$ as a function of concentration and calculate EC50 as follows: $y = A1-A2/1+e^{(x-x0)/dx} + A2$, where y is the $I_{normalized}$ at a given concentration (x), A1 and A2 are the $I_{normalizedmax}$ and $I_{normalizedmin}$, respectively, x is the given concentration, xo is the EC50, and dx is the slope factor. Microcal Origin 6.0 software was used to fit the data.

Acknowledgements

Authors contributions

SF, AJS, VN, UT, HN and MO performed experiments and analysed data; ACMO, OW and LT designed and supervised experiments and analysed data; LT, OW and ACMO wrote the paper. All authors have seen and approved the final manuscript.

Conflict of interest

The authors declare no competing financial interests.

Figure legends

Figure 1 Identification of a new SNX3 isoform and its interaction with PC2

A. Yeast 2-hybrid screens of an E17 embryonic mouse cDNA library using a portion (aa799-895) of the C-terminus of human PKD2 (CT2) as bait identified a novel isoform of SNX3. Yeast co-transformants were retested on selective media to activate HIS3 and ADE2 selection markers. The new isoform SNX3-102 interacted with CT2 (799-871) and full-length CT2 (680-968) but was unaffected by mutations (4M) disrupting the coiled-coil domain (CC2) which mediates CT2 homodimerization. In contrast, no interaction between CT2 and SNX3-162 was detected.

B. In vitro GST pull-down assays indicate that GST-SNX3-102 but not GST-SNX3-162 bound to recombinant Thio-CT2 directly. Neither GST nor glutathione beads bound to Thio-CT2.

C. Exon map showing the alternative splicing of different human isoforms of SNX3. Compared with the classic isoform SNX3-162, the new isoform SNX3-102 is missing exon 3 and part of exon 4. The PX domain region is marked by the shaded bar. Numbers indicate the amino-acid boundaries for different exons and domains. Dotted boxes represent missing exons. The two isoforms were amplified independently using specific primers indicated by arrows on the figure. The sequence targeted by the SNX3 siRNA is indicated. Swiss-Prot Accession numbers: O60493 (isoform 1); O60493-2 (isoform 2); O60493-3 (isoform 3); O60493-4 (isoform 4).

D. Ratio of SNX3-102 versus SNX3-162 in developing mouse embryos between E10 and E16. The relative mRNA level of SNX3-102 level was ~ 3-5% that of SNX3-162 (set to 100%) at each developmental stage. A similar ratio between both isoforms was found in mouse IMCD cells. Expression of murine SNX3-102 mRNA showed a trend to increase during development. The relative mRNA level was calculated in relation to that of HPRT.

Figure 2 SNX3-162 binds to the N-terminus of PC2 via the core retromer protein VPS35

A. Co-immunoprecipitation assays between full-length HA-PC2 and myc-SNX3-102 or myc-SNX3-162 in transfected HEK293 cells. Both isoforms bound to full-length PC2 in

both directions.

B. A small plasma membrane pool of GFP-SNX3-102 (70% transfected cells show membrane expression) could be visualized in MDCK II cells (arrow) whereas GFP-SNX3-162 did not show clear surface expression under same conditions (top panel). GFP-SNX3-102 co-localized with the endocytosis-associated protein AP2 (middle panel). In contrast, GFP-SNX3-162 co-localized with the early endosome marker, EEA1 (bottom panel). Similar findings were observed in HeLA, MDCK and IMCD3 cells (not shown).

C. GST pull-down assays from cell lysates showing that GST-SNX3-102 but not GST-SNX3-162 binds to endogenous clathrin and the AP2µ2 subunit. Loading controls and binding of GST fusion proteins to beads is showed in the lower panels. The doublet bands observed for AP2µ2 could represent different splice forms or phosphorylation status.

D. Co-immunoprecipitation assays between full-length HA-PC2 and full length GFP-VPS35 in transfected HEK293 cells. VPS35 bound to full-length PC2 in both directions.

E. Immunoprecipitation of endogenous PC2 by the PC2 mAb YCE2 (Santa Cruz, USA) from LLCPK1 cells co-immunoprecipitated endogenous VPS35 and SNX3 in the same complex. An irrelevant mIgG2A antibody was used as a negative control.

F. siRNA knockdown of VPS35 abolished the binding of SNX3 to endogenous PC2 in co-IP assays from LLCPK1 cells. A scrambled siRNA control had no effect on this interaction. An irrelevant mIgG2A antibody was used as a negative control for the IP.

G. GST pull-down assays from HEK293 cell lysates showing that a recombinant GST protein encoding the N-terminus of PC2 (GST-NT2, aa1-223) but not the C-terminus of PC2 (GST-CT2, aa 680-968) bound to co-expressed GFP-VPS35. Binding of the C-terminus of PC1 (GST-CT1, aa 4107-4303) to GFP-VPS35 was also detected.

H. In vitro GST binding assays using purified GST-NT2 and recombinant FLAG-VPS35/26/29-His proteins confirmed a direct interaction between both proteins. GST protein was used as a negative control.

I. In vitro binding between recombinant MBP-CT1 and recombinant FLAG-VPS35/26/29-His proteins indicate a direct interaction between the two proteins. MBP protein was used as a negative control.

Figure 3 Knockdown of SNX3 or VPS35 leads to increased surface expression of endogenous PC1 and PC2 in LLC-PK1 cells and in Xenopus pronephric tubules

A. Surface expression of endogenous PC1 and PC2 in LLC-PK1 cells was increased following selective knockdown of SNX3 or VPS35 siRNA (20nM) compared to a scrambled control siRNA. Surface biotinylated PC1 and PC2 was compared to total PC1/PC2. Na^+-K^+-ATPase and calnexin were used as positive and negative controls respectively for surface biotinylation.

B. The ratio of biotinylated/total PC1 calculated from four independent experiments showed a significant increase following SNX3 ($p<0.05$) and VPS35 ($P<0.05$) knockdown: Scrambled siRNA = 0.139 ± 0.047; SNX3 siRNA = 0.306 ± 0.048; VPS35 siRNA = 0.600 ± 0.171. Similarly, a significant increase in biotinylated PC2 was observed following SNX3 ($p<0.05$) and VPS35 ($P<0.001$) knockdown in triplicate experiments: Scrambled siRNA = 0.235 ± 0.035; SNX3 siRNA = 0.527 ± 0.076; VPS35 siRNA = 1.289 ± 0.038. The increase in biotinylated PC1 and PC2 was quantitatively greater following VPS35 knockdown compared to SNX3 despite a more complete inhibition of the latter.

C. EndoH digestion of surface biotinylated proteins in LLCPK1 cells. While PC1 and Na^+ K^+ ATPase were EndoH resistant, surface labelled PC2 was EndoH sensitive. Calnexin, an ER resident protein acts as a negative control for the biotinylation assay. Representative experiment of two shown.

D. Endogenous PC2 expression in LLC-PK1 cells detected by widefield immunofluorescence microscopy using a specific PC2 antibody (g20, Santa Cruz, USA) as previously described [18]. A proportion of PC2 was detectable in the lateral plasma membrane as well as in primary cilia co-labelled with an antibody to acetylated tubulin (arrows). Left - A clear increase in plasma membrane PC2 staining was observed following knockdown of SNX3 or VPS35 relative to untransfected controls or cells transfected with a scrambled siRNA. Right - No change in cilia PC2 expression was detectable. Images are representative of 3 separate experiments.

E. Surface staining intensity was calculated as a percentage relative to control untransfected cells and expressed as bar diagrams. Left - A significant increase in surface expression of PC2 was seen following SNX3 and VPS35 knockdown ($p<0.005$):

Scrambled siRNA = -5.54% ± 1.68, n=30; SNX3 siRNA = 14.74% ± 4.24, n=30; VPS35 siRNA = 35.01% ± 2.28, n=30. Right - there was no significant difference in cilia localization of PC2: control siRNA = 92.88 ± 4.52, n=50; Scrambled siRNA = 92.42% ± 7.58, n=32; SNX3 siRNA = 93.3% ± 3.88, n=31; VPS35 siRNA = 96.43% ± 3.57, n=39.

F. Uninjected Xenopus controls (i, ii) and embryos injected unilaterally with a total of 1.6 pmol Vps34-MO (iii, iv) were analyzed at stage 40 by PC2 immunofluorescence (red). ECL was used to visualize the apical side of the proximal tubules (green) and nuclei were counterstained with DAPI (blue). Images were analyzed by confocal microscopy and all three z-planes are shown. The white lines indicate the position used for x,z and y,z planes, respectively.

G. Bar diagram to quantify the apical pixel intensity of PC2 staining. Error bars represent standard deviation and statistical significance was determined using Student's t-test (* p<0.05). Note that the pronephric tubules of Vps35 morphants are dilated, which is likely due to the effect of the retromer complex on the secretion of Wnt ligands and their role in kidney tubulogenesis [11, 26].

Figure 4 Depletion of VPS35 increases functional expression of PC2

A-L. Current-voltage (I-V, A,D,G, and J), time course (B,E,H, and K), and representative step whole cell currents (C,F,I,I, and L) in cells transfected with a scrambled control siRNA (mock, n=6, A), PC2-specific siRNA (n=8, B), VPS35-specific siRNA (n=10, C), or VPS35- and PC2-specific siRNAs (n=8, D) in the presence (red IV-curves) or absence (black I-V curves) of 500ng/ml Wnt9b in the extracellular solution. Outward currents are shown in blue and inward currents are shown in black in time course experiments. Currents were blocked by the addition of 100 μM La^{3+} added in the extracellular solution at the indicated time points. I-V curves were taken at 4-5 min after the addition of Wnt9b, when currents were stable and towards the end of each pulse (195 ms).

M-N. Summary data of outward (M, at +100mV, blue) and inward current densities (N, -100mV, black) in all four groups. **, indicates p<0.001, ***, indicates p<0.0005.

(O). Total cell capacitance in pF in all four groups. ns, indicates p>0.005

Figure 5 Model of SNX3 and retromer regulated PC1/PC2 trafficking and recycling to the PM

A sequential model of PC2 sorting by the two SNX3 isoforms is displayed. SNX3-102 mediates surface PC2 retrieval and clustering in clathrin-coated vesicles by binding both to surface PC2 and AP2/clathrin. A direct interaction between PC1 and AP2/ARRB1 mediated through the PLAT domain has also been reported [41]. PC1/ PC2 are then delivered to early endosomes where they can bind to SNX3-162 indirectly via VPS35 to the retromer complex. Sorting of different pools of endosomal PC1/PC2 for recycling to the plasma membrane, retrograde transport to the TGN (retromer) or to lysosomes for degradation takes place here.
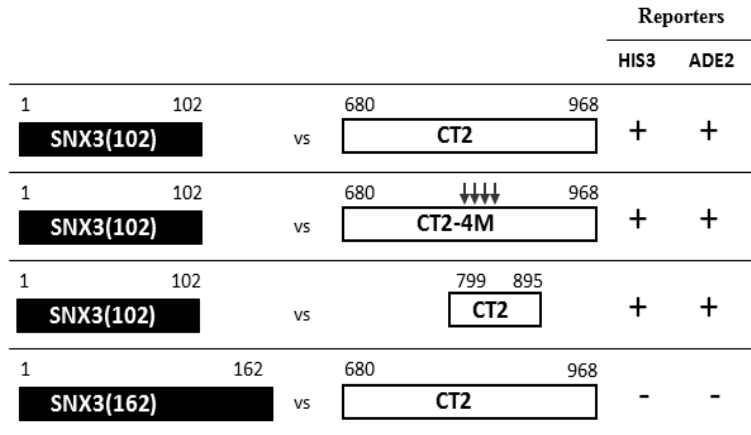
References

1. Harris, PC, Torres, VE: Genetic mechanisms and signaling pathways in autosomal dominant polycystic kidney disease. J Clin Invest, 124**:** 2315-2324, 2014.

2. Ong, AC, Harris, PC: A polycystin-centric view of cyst formation and disease: the polycystins revisited. Kidney Int, 88**:** 699-710, 2015.

3. Tsiokas, L, Kim, E, Arnould, T, Sukhatme, VP, Walz, G: Homo- and heterodimeric interactions between the gene products of PKD1 and PKD2. Proc Natl Acad Sci U S A, 94**:** 6965-6970, 1997.

4. Newby, LJ, Streets, AJ, Zhao, Y, Harris, PC, Ward, CJ, Ong, AC: Identification, characterization, and localization of a novel kidney polycystin-1-polycystin-2 complex. J Biol Chem, 277**:** 20763-20773, 2002.

5. Giamarchi, A, Feng, S, Rodat-Despoix, L, Xu, Y, Bubenshchikova, E, Newby, LJ, Hao, J, Gaudioso, C, Crest, M, Lupas, AN, Honore, E, Williamson, MP, Obara, T, Ong, AC, Delmas, P: A polycystin-2 (TRPP2) dimerization domain essential for the function of heteromeric polycystin complexes. EMBO J, 29**:** 1176-1191, 2010.

6. Ong, AC, Harris, PC: Molecular pathogenesis of ADPKD: The polycystin complex gets complex. Kidney Int, 67**:** 1234-1247, 2005.

7. Bai, CX, Giamarchi, A, Rodat-Despoix, L, Padilla, F, Downs, T, Tsiokas, L, Delmas, P: Formation of a new receptor-operated channel by heteromeric assembly of TRPP2 and TRPC1 subunits. EMBO Rep, 9**:** 472-479, 2008.

8. Kottgen, M, Buchholz, B, Garcia-Gonzalez, MA, Kotsis, F, Fu, X, Doerken, M, Boehlke, C, Steffl, D, Tauber, R, Wegierski, T, Nitschke, R, Suzuki, M, Kramer-Zucker, A, Germino, GG, Watnick, T, Prenen, J, Nilius, B, Kuehn, EW, Walz, G: TRPP2 and TRPV4 form a polymodal sensory channel complex. J Cell Biol, 182**:** 437-447, 2008.

9. Zhang, ZR, Chu, WF, Song, B, Gooz, M, Zhang, JN, Yu, CJ, Jiang, S, Baldys, A, Gooz, P, Steele, S, Owsianik, G, Nilius, B, Komlosi, P, Bell, PD: TRPP2 and TRPV4 form an EGF-activated calcium permeable channel at the apical membrane of renal collecting duct cells. PLoS One, 8**:** e73424, 2013.

10. Du, J, Ma, X, Shen, B, Huang, Y, Birnbaumer, L, Yao, X: TRPV4, TRPC1, and TRPP2 assemble to form a flow-sensitive heteromeric channel. FASEB J, 28**:** 4677-4685, 2014.

11. Kim, S, Nie, H, Nesin, V, Tran, U, Outeda, P, Bai, CX, Keeling, J, Maskey, D, Watnick, T, Wessely, O, Tsiokas, L: The polycystin complex mediates Wnt/Ca(2+) signalling. Nat Cell Biol, 18**:** 752-764, 2016.

12. Cai, Y, Anyatonwu, G, Okuhara, D, Lee, KB, Yu, Z, Onoe, T, Mei, CL, Qian, Q, Geng, L, Wiztgall, R, Ehrlich, BE, Somlo, S: Calcium dependence of polycystin-2 channel activity is modulated by phosphorylation at Ser812. J Biol Chem, 279**:** 19987-19995, 2004.

13. Mekahli, D, Sammels, E, Luyten, T, Welkenhuyzen, K, van den Heuvel, LP, Levtchenko, EN, Gijsbers, R, Bultynck, G, Parys, JB, De Smedt, H, Missiaen, L: Polycystin-1 and polycystin-2 are both required to amplify inositol-trisphosphate-induced Ca(2+) release. Cell calcium, 2012.

14. Li, Y, Santoso, NG, Yu, S, Woodward, OM, Qian, F, Guggino, WB: Polycystin-1

interacts with inositol 1,4,5-trisphosphate receptor to modulate intracellular Ca2+ signaling with implications for polycystic kidney disease. J Biol Chem, 284**:** 36431-36441, 2009.

15. Gonzalez-Perret, S, Kim, K, Ibarra, C, Damiano, AE, Zotta, E, Batelli, M, Harris, PC, Reisin, IL, Arnaout, MA, Cantiello, HF: Polycystin-2, the protein mutated in autosomal dominant polycystic kidney disease (ADPKD), is a Ca2+-permeable nonselective cation channel. Proc Natl Acad Sci U S A, 98**:** 1182-1187, 2001.

16. Kottgen, M, Benzing, T, Simmen, T, Tauber, R, Buchholz, B, Feliciangeli, S, Huber, TB, Schermer, B, Kramer-Zucker, A, Hopker, K, Simmen, KC, Tschucke, CC, Sandford, R, Kim, E, Thomas, G, Walz, G: Trafficking of TRPP2 by PACS proteins represents a novel mechanism of ion channel regulation. EMBO J, 24**:** 705-716, 2005.

17. Streets, AJ, Wessely, O, Peters, DJ, Ong, AC: Hyperphosphorylation of polycystin-2 at a critical residue in disease reveals an essential role for polycystin-1-regulated dephosphorylation. Human molecular genetics, 22**:** 1924-1939, 2013.

18. Streets, AJ, Moon, DJ, Kane, ME, Obara, T, Ong, AC: Identification of an N-terminal glycogen synthase kinase 3 phosphorylation site which regulates the functional localization of polycystin-2 in vivo and in vitro. Hum Mol Genet, 15**:** 1465-1473, 2006.

19. Streets, AJ, Needham, AJ, Gill, SK, Ong, AC: Protein kinase D-mediated phosphorylation of polycystin-2 (TRPP2) is essential for its effects on cell growth and calcium channel activity. Molecular biology of the cell, 21**:** 3853-3865, 2010.

20. Xu, Y, Hortsman, H, Seet, L, Wong, SH, Hong, W: SNX3 regulates endosomal function through its PX-domain-mediated interaction with PtdIns(3)P. Nature cell biology, 3**:** 658-666, 2001.

21. Mizutani, R, Yamauchi, J, Kusakawa, S, Nakamura, K, Sanbe, A, Torii, T, Miyamoto, Y, Tanoue, A: Sorting nexin 3, a protein upregulated by lithium, contains a novel phosphatidylinositol-binding sequence and mediates neurite outgrowth in N1E-115 cells. Cell Signal, 21**:** 1586-1594, 2009.

22. Luo, Y, Vassilev, PM, Li, X, Kawanabe, Y, Zhou, J: Native polycystin 2 functions as a plasma membrane ca(2+)-permeable cation channel in renal epithelia. Mol Cell Biol, 23**:** 2600-2607, 2003.

23. Tsiokas, L: Function and regulation of TRPP2 at the plasma membrane. Am J Physiol Renal Physiol, 297**:** F1-9, 2009.

24. Tran, U, Zakin, L, Schweickert, A, Agrawal, R, Doger, R, Blum, M, De Robertis, EM, Wessely, O: The RNA-binding protein bicaudal C regulates polycystin 2 in the kidney by antagonizing miR-17 activity. Development, 137**:** 1107-1116, 2010.

25. Tran, U, Pickney, LM, Ozpolat, BD, Wessely, O: Xenopus Bicaudal-C is required for the differentiation of the amphibian pronephros. Developmental biology, 307**:** 152-164, 2007.

26. Coudreuse, DY, Roel, G, Betist, MC, Destree, O, Korswagen, HC: Wnt gradient formation requires retromer function in Wnt-producing cells. Science, 312**:** 921-924, 2006.

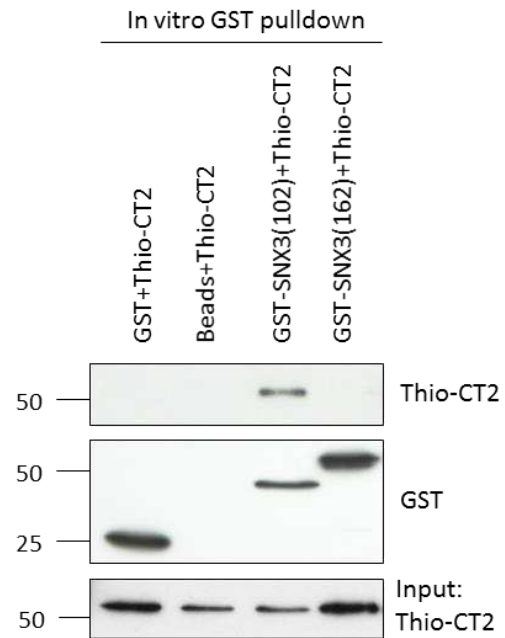27. Wang, Q, Yin, H, He, J, Ye, J, Ding, F, Wang, S, Hu, X, Meng, Q, Li, N: cDNA cloning

of porcine PKD2 gene and RNA interference in LLC-PK1 cells. Gene, 476**:** 38-45, 2011.

28. McGough, IJ, Cullen, PJ: Recent advances in retromer biology. Traffic, 12**:** 963-971, 2011.

29. Borner, GH, Harbour, M, Hester, S, Lilley, KS, Robinson, MS: Comparative proteomics of clathrin-coated vesicles. J Cell Biol, 175**:** 571-578, 2006.

30. Chiow, KH, Tan, Y, Chua, RY, Huang, D, Ng, ML, Torta, F, Wenk, MR, Wong, SH: SNX3-dependent regulation of epidermal growth factor receptor (EGFR) trafficking and degradation by aspirin in epidermoid carcinoma (A-431) cells. Cell Mol Life Sci, 69**:** 1505-1521, 2012.

31. Strochlic, TI, Schmiedekamp, BC, Lee, J, Katzmann, DJ, Burd, CG: Opposing activities of the Snx3-retromer complex and ESCRT proteins mediate regulated cargo sorting at a common endosome. Mol Biol Cell, 19**:** 4694-4706, 2008.

32. Harterink, M, Port, F, Lorenowicz, MJ, McGough, IJ, Silhankova, M, Betist, MC, van Weering, JR, van Heesbeen, RG, Middelkoop, TC, Basler, K, Cullen, PJ, Korswagen, HC: A SNX3-dependent retromer pathway mediates retrograde transport of the Wnt sorting receptor Wntless and is required for Wnt secretion. Nature cell biology, 13**:** 914-923, 2011.

33. Hoffmeister, H, Babinger, K, Gurster, S, Cedzich, A, Meese, C, Schadendorf, K, Osten, L, de Vries, U, Rascle, A, Witzgall, R: Polycystin-2 takes different routes to the somatic and ciliary plasma membrane. J Cell Biol, 192**:** 631-645, 2011.

34. Nigro, EA, Castelli, M, Boletta, A: Role of the Polycystins in Cell Migration, Polarity, and Tissue Morphogenesis. Cells, 4**:** 687-705, 2015.

35. Follit, JA, San Agustin, JT, Xu, F, Jonassen, JA, Samtani, R, Lo, CW, Pazour, GJ: The Golgin GMAP210/TRIP11 anchors IFT20 to the Golgi complex. PLoS Genet, 4**:** e1000315, 2008.

36. Follit, JA, Tuft, RA, Fogarty, KE, Pazour, GJ: The intraflagellar transport protein IFT20 is associated with the Golgi complex and is required for cilia assembly. Mol Biol Cell, 17**:** 3781-3792, 2006.

37. Yu, S, Hackmann, K, Gao, J, He, X, Piontek, K, Garcia Gonzalez, MA, Menezes, LF, Xu, H, Germino, GG, Zuo, J, Qian, F: Essential role of cleavage of Polycystin-1 at G protein-coupled receptor proteolytic site for kidney tubular structure. Proc Natl Acad Sci U S A, 104**:** 18688-18693, 2007.

38. Kim, H, Xu, H, Yao, Q, Li, W, Huang, Q, Outeda, P, Cebotaru, V, Chiaravalli, M, Boletta, A, Piontek, K, Germino, GG, Weinman, EJ, Watnick, T, Qian, F: Ciliary membrane proteins traffic through the Golgi via a Rabep1/GGA1/Arl3-dependent mechanism. Nat Commun, 5**:** 5482, 2014.

39. Delling, M, Indzhykulian, AA, Liu, X, Li, Y, Xie, T, Corey, DP, Clapham, DE: Primary cilia are not calcium-responsive mechanosensors. Nature, 531**:** 656-660, 2016.

40. Gainullin, VG, Hopp, K, Ward, CJ, Hommerding, CJ, Harris, PC: Polycystin-1 maturation requires polycystin-2 in a dose-dependent manner. J Clin Invest, 2015.

41. Xu, Y, Streets, AJ, Hounslow, AM, Tran, U, Jean-Alphonse, F, Needham, AJ, Vilardaga, JP, Wessely, O, Williamson, MP, Ong, AC: The Polycystin-1, Lipoxygenase, and alpha-Toxin Domain Regulates Polycystin-1 Trafficking. J Am Soc Nephrol, 27**:**

1159-1173, 2016.

42. Feng, S, Okenka, GM, Bai, CX, Streets, AJ, Newby, LJ, Dechant, BT, Tsiokas, L, Obara, T, Ong, AC: Identification and Functional Characterization of an N-terminal Oligomerization Domain for Polycystin-2. J Biol Chem, 283**:** 28471-28479, 2008.

43. Tabuchi, M, Yanatori, I, Kawai, Y, Kishi, F: Retromer-mediated direct sorting is required for proper endosomal recycling of the mammalian iron transporter DMT1. Journal of cell science, 123**:** 756-766, 2010.

44. Sive, HL, Grainger, RM, Harland, RM: Early Development of Xenopus leavis: a Laboratory Manual. Cold Spring Harbor, New York: Cold Spring Harbor Laboratory Press, 2000.

45. Nieuwkoop, PD, Faber, J: Normal Table of Xenopus laevis. New York: Garland Publishing, 1994.

46. Cerqueira, DM, Tran, U, Romaker, D, Abreu, JG, Wessely, O: Sterol carrier protein 2 regulates proximal tubule size in the Xenopus pronephric kidney by modulating lipid rafts. Dev Biol, 394**:** 54-64, 2014.
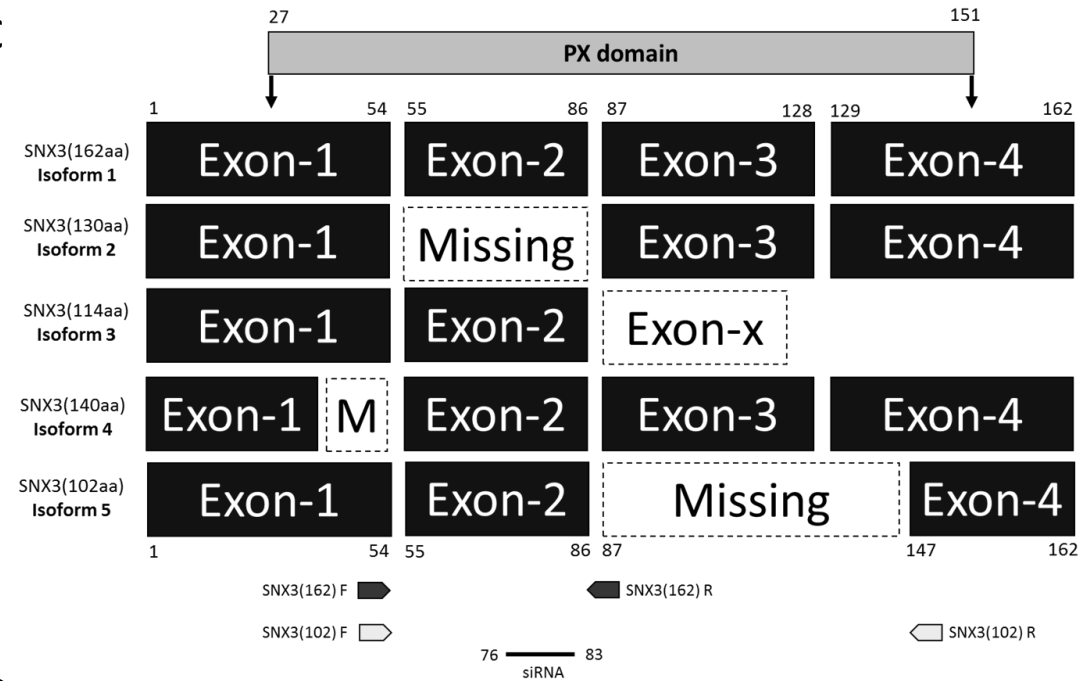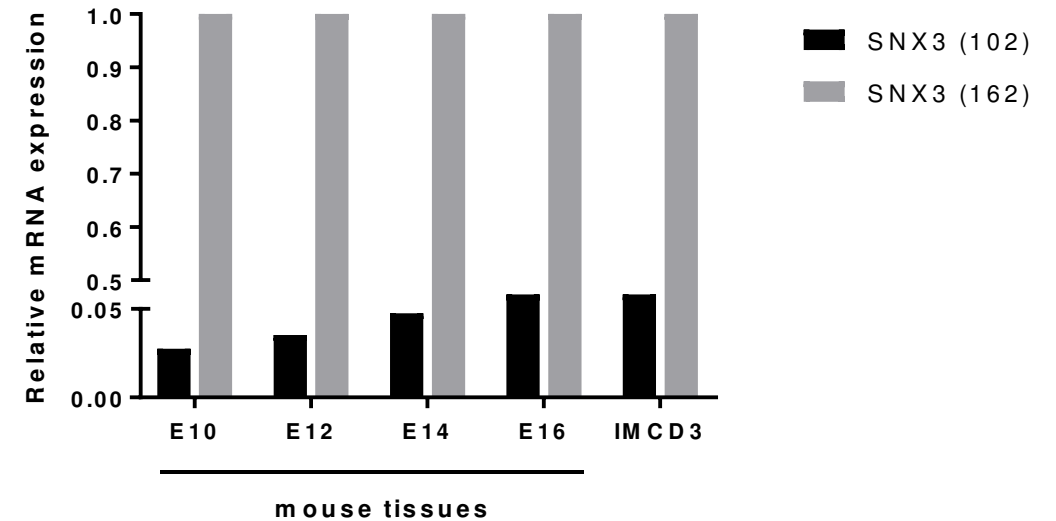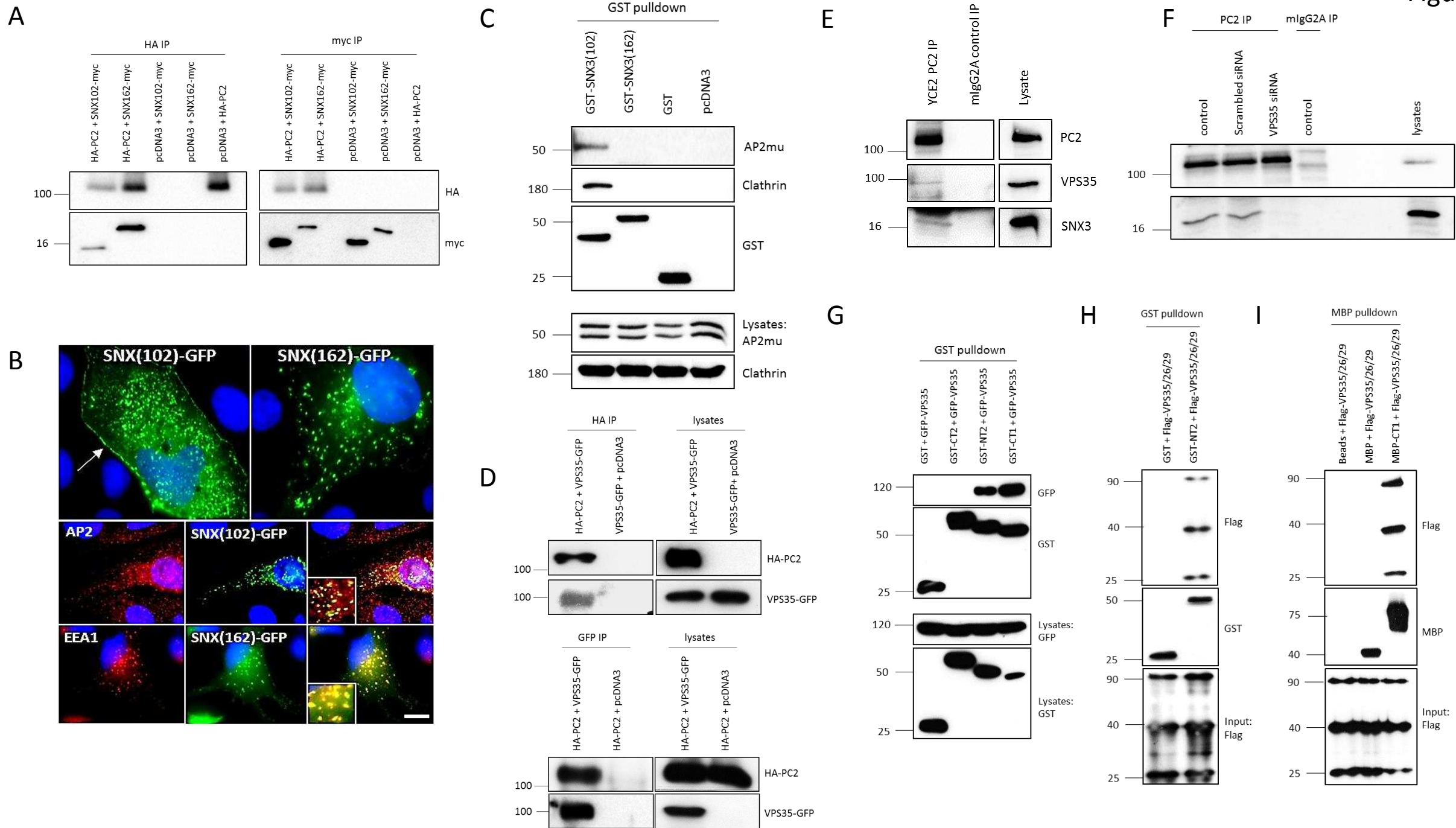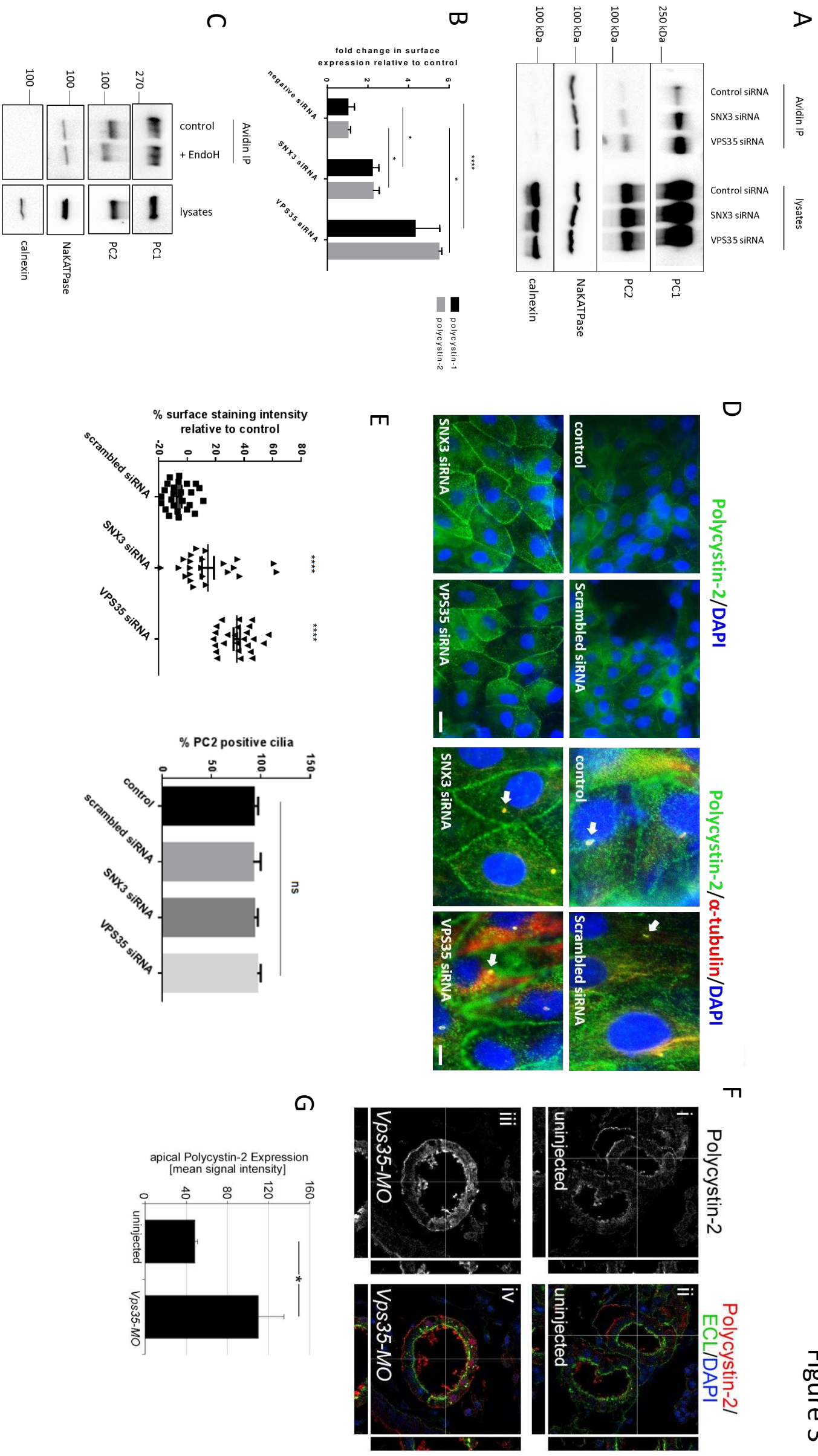
Figure 1

Figure 2

Figure 3

Figure 4

Figure 5

PC2 endocytosis is mediated by SNX(102)
PC1 endocytosis is mediated by ARRB1/2
(Xu et al JASN 2015)

SNX3(102)

SNX3(102)
AP2   PC2   PC1   ARRB1

PC2   PC1
SNX3(102)   ARRB1
PC2 binds to isoform 5 of SNX3

Endocytic vesicle

PC2   PC1

Early recycling endosome

PC2   PC1
PC1/PC2 is recycled to the plasma membrane

VPS29
VPS35
VPS 26   PC2   PC1
SNX3(162)
PI3P
PC1/PC2 binds to the retromer complex

Early endosome

Golgi apparatus

ER

PC2   PC1
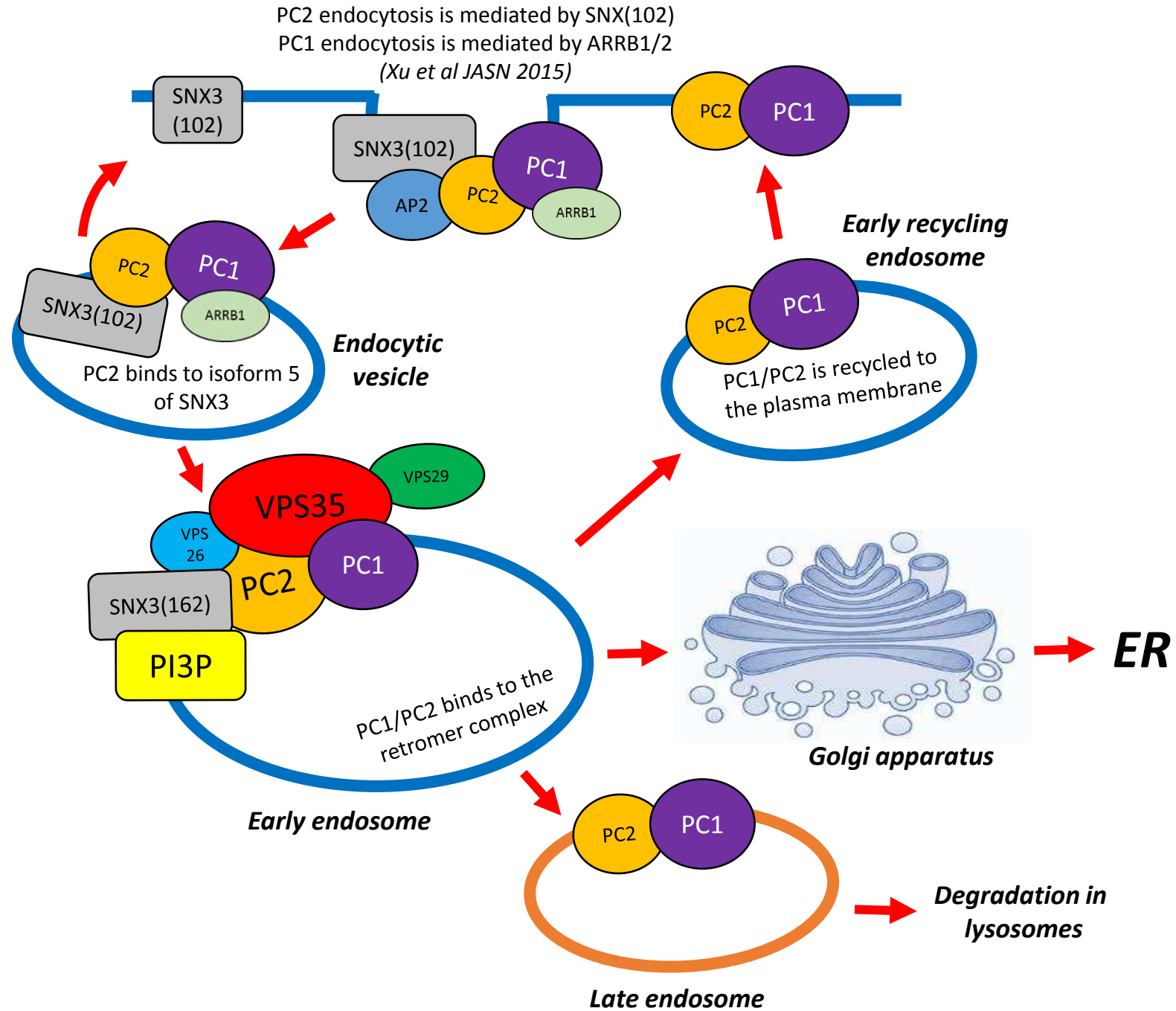
Late endosome

Degradation in lysosomes

Supplementary Figures

S. Figure-1 Sequence analysis of novel isoform SNX3(102).

A. Nucleotide sequence of mouse SNX-162 isoform 1 (RefSeq: NM_017472) with amino acid translation (RefSeq: NP_059500, UniProt: Q78ZM0). Alternating exons are depicted in blue.

B. Nucleotide sequence of the novel mouse SNX3-102 isoform isolated and sequenced from an E17 embryonic mouse cDNA library with amino acid translation. The cryptic splice site AAG/G is underlined in bold.

S. Figure-2 Knockdown of SNX-3, VPS35 or Pkd2 in LLC-PK1 and Xenopus

A. Protein-lipid overlay assays showing that SNX3-102 does not bind PtdIns(3)P unlike SNX3-162 due to the truncation of the PX domain.

B. Knockdown of SNX3-102 and SNX3-162 by siRNA in LLC-PK1 cells quantified by RT-PCR. Actin was used as a negative control.

C. Ratio of SNX3-102 versus SNX3-162 in several human cell lines. The relative mRNA level of SNX3-102 level was ~ 3-5% that of SNX3-162. The relative mRNA level was calculated in relation to that of HPRT. UCL93 was derived from normal human kidney whereas OX161 was generated from an ADPKD kidney [47].

D,E. LLC-PK1 cells transfected with 20 nM siRNA targeting SNX3-162 or VPS35 showing specific knockdown compared to control untransfected cells and cells transfected with non-targeting scrambled siRNA. Equal loading is confirmed by probing the same membrane for actin expression.

S. Figure-3 PC2 localisation in *Xenopus* proximal tubules is regulated by Vps35 expression

A. Specificity of PC2 localization in *Xenopus* proximal tubules. The apical surface was labelled with ECL. PC2 localization was detected at both apical and basolateral membranes and markedly reduced after injection of a *Pkd2-MO*.

B. PC2 surface localization in *Xenopus* proximal tubules was altered by a VPS35-MO but not a control (Std) MO.

C. VPS35 knockdown in *Xenopus* embryos with a specific MOs confirmed by immunoblotting with a VPS35 antibody in two independent batches of embryos (3 pooled per lane). γ tubulin was used as loading control.

S. Figure-4 Expression of PC1 and dose-response curves to Wnt5a and Wnt9b in LLC-PK1 cells

A. PC1 expression in LLCPK-1 cells detected by immunoblotting with a monoclonal anti-PC1 antibody (7e12) using 50 (lane 1) or 100 μg (lane 2) of total protein.

B. Boltzmann curves of normalised currents in LLCPK-1 cells after Wnt5a and Wnt9b stimulation at two different voltages (-100mV and +100mV). EC50 values for Wnt5a are 76 ng/ml (-100 mV) and 49 ng/ml (+100 mV). EC50 values for Wnt9b are 74 ng/ml (-100 mV) and 45 ng/ml (+100 mV).

A

```
M.Mus SNX3(162) Isoform 1

  1 ATGGCGGAGACGGTAGCGGACACCCGGCGGCTCATCACCAAGCCGCAGAATCTGAATGAC
  1 -M--A--E--T--V--A--D--T--R--R--L--I--T--K--P--Q--N--L--N--D-

 61 GCCTACGGGCCGCCCAGCAACTTCCTCGAGATCGACGTGAGCAACCCGCAGACCGTGGGG
 21 -A--Y--G--P--P--S--N--F--L--E--I--D--V--S--N--P--Q--T--V--G-

121 GTCGGCCGGGGCCGCTTCACCACCTACGAGATCAGGGTCAAGACAAATCTTCCTATCTTC
 41 -V--G--R--G--R--F--T--T--Y--E--I--R--V--K--T--N--L--P--I--F-

181 AAGCTGAAGGAATCTACTGTTAGAAGAAGATACAGTGACTTTGAGTGGCTTCGAAGTGAA
 61 -K--L--K--E--S--T--V--R--R--R--Y--S--D--F--E--W--L--R--S--E-

241 CTAGAAAGAGAGAGCAAGGTTGTAGTTCCCCCACTCCCTGGGAAAGCATTTTTGCGGCAG
 81 -L--E--R--E--S--K--V--V--V--P--P--L--P--G--K--A--F--L--R--Q-

301 CTTCCTTTTAGAGGAGACGATGGAATATTTGATGACAATTTCATCGAGGAAAGGAAGCAA
101 -L--P--F--R--G--D--D--G--I--F--D--D--N--F--I--E--E--R--K--Q-

361 GGGCTGGAACAGTTCATAAACAAGGTCGCTGGTCATCCTCTGGCCCAGAATGAACGTTGT
121 -G--L--E--Q--F--I--N--K--V--A--G--H--P--L--A--Q--N--E--R--C-

421 CTTCACATGTTTTTACAGGATGAAATTATAGATAAAAGCTATACTCCATCTAAAATAAGA
141 -L--H--M--F--L--Q--D--E--I--I--D--K--S--Y--T--P--S--K--I--R-

481 CATGCCTGA
161 -H--A--*-
```

B

```
M.mus SNX3(102) Novel Isoform

  1 ATGGCGGAGACGGTAGCGGACACCCGGCGGCTCATCACCAAGCCGCAGAATCTGAATGAC
  1 -M--A--E--T--V--A--D--T--R--R--L--I--T--K--P--Q--N--L--N--D-

 61 GCCTACGGGCCGCCCAGCAACTTCCTCGAGATCGACGTGAGCAACCCGCAGACCGTGGGG
 21 -A--Y--G--P--P--S--N--F--L--E--I--D--V--S--N--P--Q--T--V--G-

121 GTCGGCCGGGGCCGCTTCACCACCTACGAGATCAGGGTCAAGACAAATCTTCCTATCTTC
 41 -V--G--R--G--R--F--T--T--Y--E--I--R--V--K--T--N--L--P--I--F-

181 AAGCTGAAGGAATCTACTGTTAGAAGAAGATACAGTGACTTTGAGTGGCTTCGAAGTGAA
 61 -K--L--K--E--S--T--V--R--R--R--Y--S--D--F--E--W--L--R--S--E-

241 CTAGAAAGAGAGAGCAAGGATGAAATTATAGATAAAAGCTATACTCCATCTAAAATAAGA
 81  L   E   R   E   S   K   D   E   I   I   D   K   S   Y   T   P   S   K   I   R

301 CATGCCTGA
101  H   A   *
```
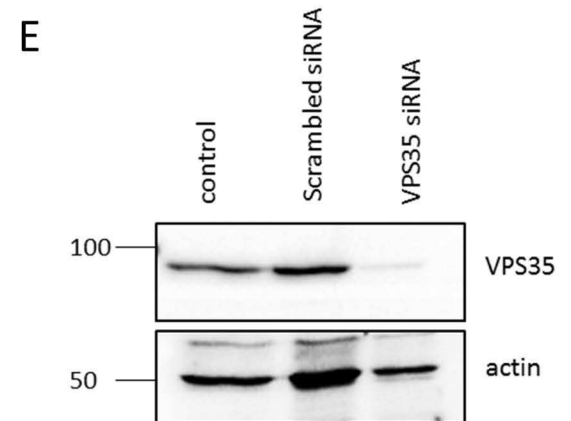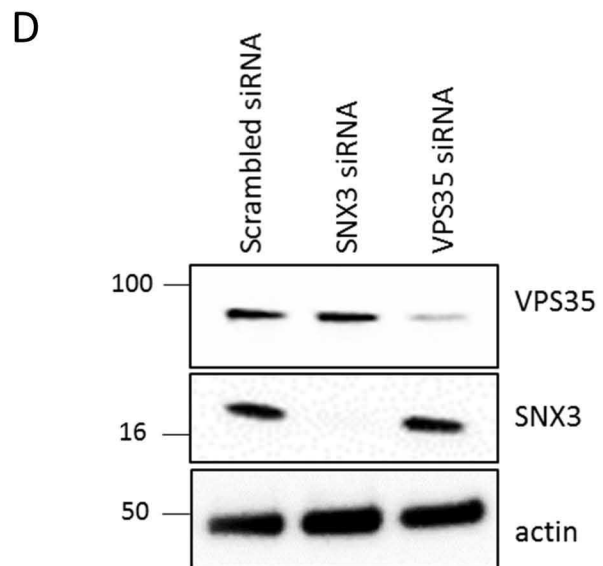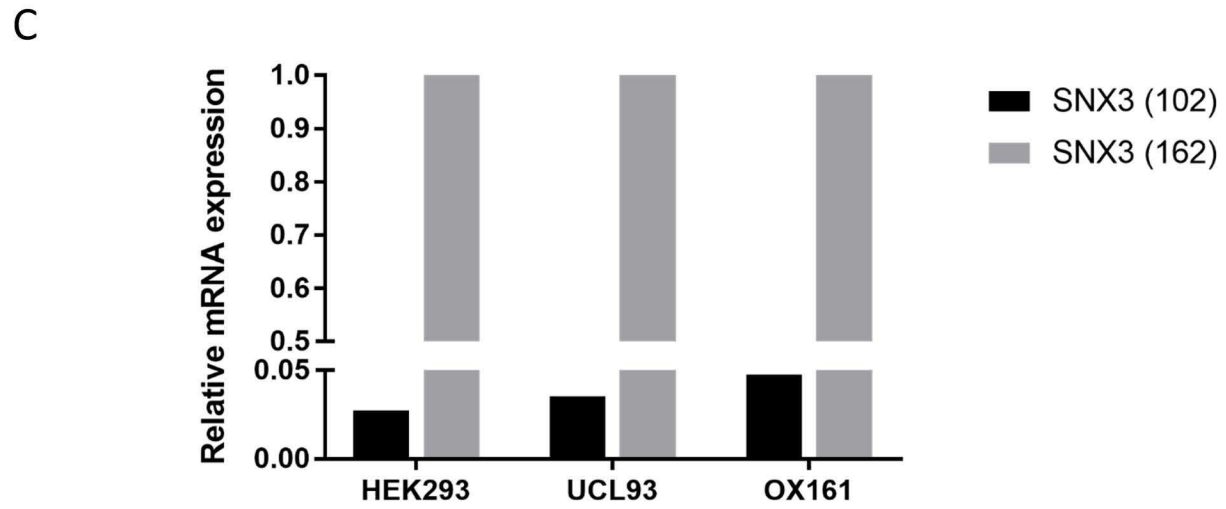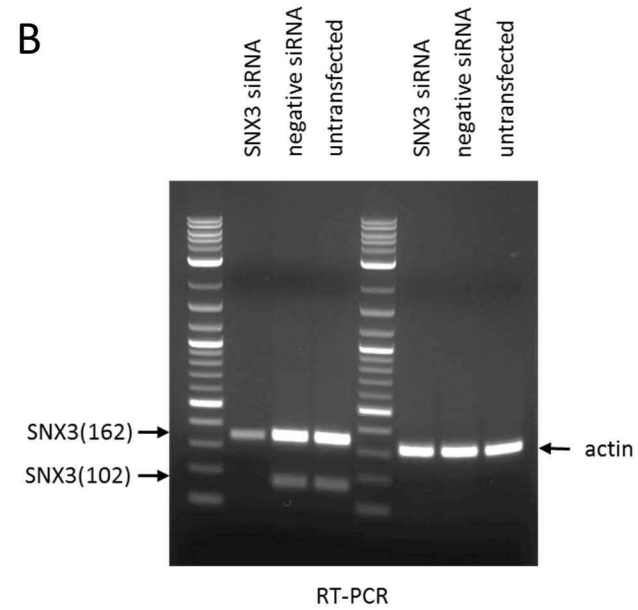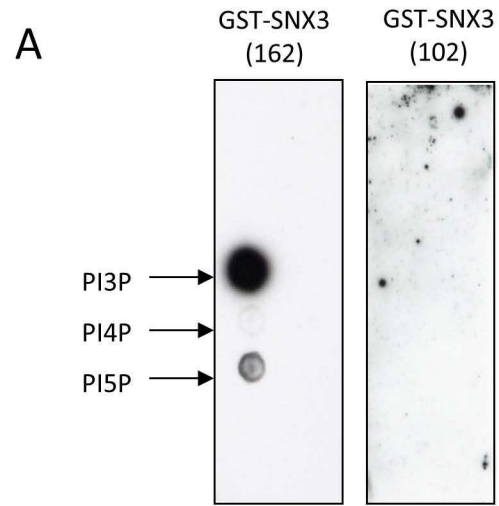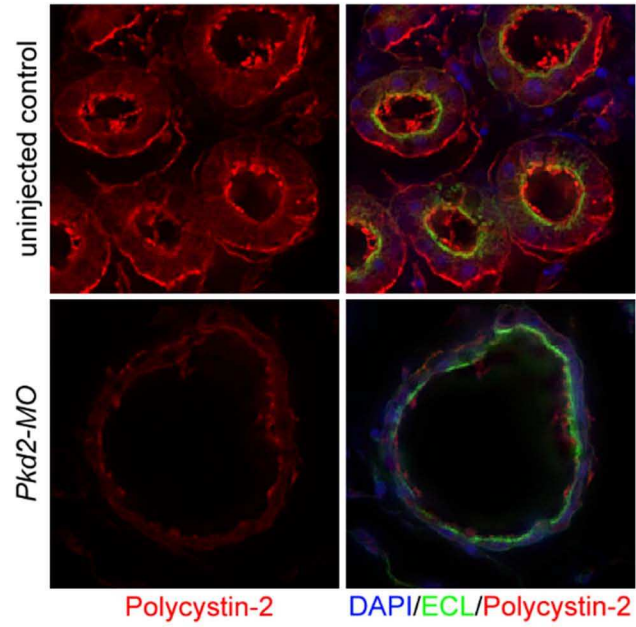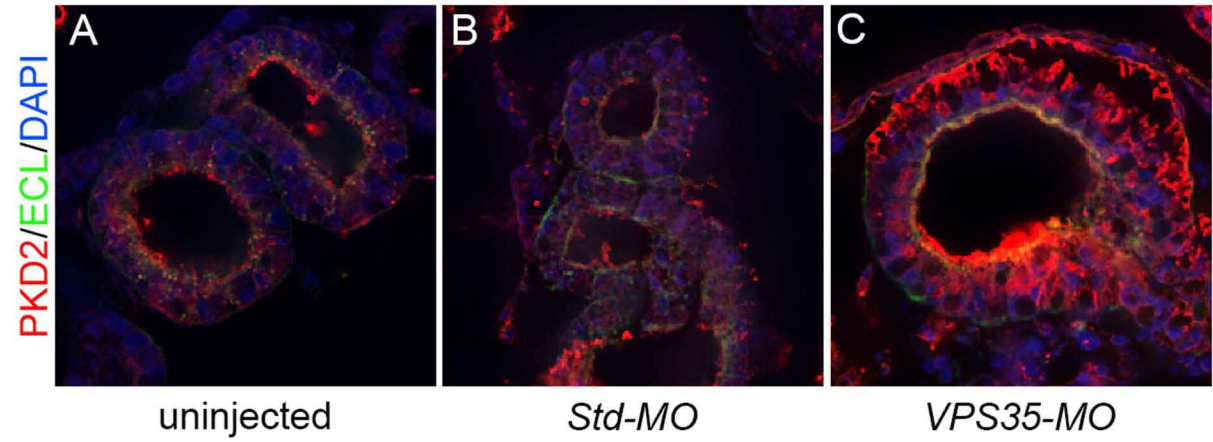**Cryptic splice site underlined in bold (AAG/G)**

A

uninjected control

Pkd2-MO

Polycystin-2   DAPI/ECL/Polycystin-2

B

PKD2/ECL/DAPI

A   B   C

uninjected   Std-MO   VPS35-MO

C

uninjected #1
uninjected #2
Vps35-MO #1
Vps35-MO #2

100 —

VPS35

50 —

γ-Tubulin

A

<u>LLCPK1</u>
50 μg   100 μg

PC1 (7e12)

250

B

-100 mV (WNT 5A)

$I_{normalized}$

Lg Concentration (ng/ml)

+100 mV (WNT 5A)

$I_{normalized}$

Lg Concentration (ng/ml)

-100 mV (WNT 9B)

$I_{normalized}$

Lg Concentration (ng/ml)

+100 mV (WNT 9B)

$I_{normalized}$

Lg Concentration (ng/ml)